STUDYING MATTER EFFECTS IN VERY LONG BASELINE NEUTRINO OSCILLATION EXPERIMENTS

S. T. PETCOV [a]

Scuola Internazionale Superiore di Studi Avanzati, and
INFN - Sezione de Trieste, I-34014 Trieste, Italy

ABSTRACT

Assuming that intense neutrino and antineutrino beams will become available in so–called neutrino factories, we show that in the case of three-neutrino mixing, the very long baseline neutrino oscillation experiments will be capable to verify and test the MSW effect, to measure the lepton mixing angle θ_{13} with a relatively high precision and to determine the sign of the neutrino mass-squared difference, $\Delta m^2_{\rm atm}$, characterizing the oscillations of the atmospheric ν_μ and $\bar{\nu}_\mu$. This can be achieved by studying $\nu_e \to \nu_\mu$ and $\bar{\nu}_e \to \bar{\nu}_\mu$ oscillations which lead to matter enhancements and suppressions of wrong sign muon rates. We discuss the subleading Δm^2_{21} effects in the case of the LMA MSW solution of the solar problem, showing that they are small for $L \gtrsim 7000$ km. For shorter baselines, Δm^2_{21} effects can be relevant and their dependence on L offers a further handle for the simultaneous determination of the CP-violation phase δ and of θ_{13}. Our results suggest that the very long baseline experiments should be performed at two distances, at $L \sim 3000$ km and $L \sim 7000$ km.

1. Introduction

Within the framework of three-neutrino mixing we discuss in this article the potential to verify and test the MSW effect [1)], to measure or limit the neutrino mixing angle θ_{13}, and to determine the sign of $\Delta m^2_{\rm atm}$, characterizing the oscillations [2)] of the atmospheric ν_μ and $\bar{\nu}_\mu$, in terrestrial very long baseline experiments with neutrino factories [b]. The neutrino factories can produce high intensity neutrino fluxes whose absolute values and spectra are known with relatively high precision and thus can be under control [4)].

Demonstrating and testing the MSW effect directly is of significant importance since this effect is supposed to play a fundamental role in many physics phenomena involving neutrinos. The effect is at the basis of our understanding of the results of the solar and atmospheric neutrino experiments. The three widely discussed solutions of the solar neutrino problem - the large mixing angle (LMA) and the small mixing angle (SMA) MSW, and the LOW-quasi-vacuum oscillation (QVO) solutions (see, e.g., [5,6,7)]), correspond to transitions of solar neutrinos in which, e.g., the solar matter effects play a significant or non-negligible role. The conclusion that the

[a] Also at: INRNE, Bulgarian Academy of Sciences, 1789 Sofia, Bulgaria.

[b] The present article is based on the joint publication [3)] with M. Freund, M. Lindner and A. Romanino.

two- transitions of the atmospheric ν_μ and $\bar{\nu}_\mu$ into sterile neutrinos are strongly disfavored (if not excluded) by the atmospheric neutrino data [8], relies on the calculated magnitude of the Earth matter effects in these transitions.

The (sub-leading) $\nu_\mu \to \nu_e$ or $\bar{\nu}_\mu \to \bar{\nu}_e$ transitions of the (atmospheric) ν_μ or $\bar{\nu}_\mu$, as well as the transitions $\nu_e \to \nu_\mu$ or $\bar{\nu}_e \to \bar{\nu}_\mu$, can be strongly amplified by the Earth matter effect when neutrinos cross just the Earth mantle [1] or the Earth core [9]. This is crucial for the possibilities to measure or obtain stringent upper limits on the neutrino mixing angle θ_{13} which controls the indicated transitions. It offers also the opportunity to determine the sign of $\Delta m^2_{\rm atm}$ [3,10] which characterizes the dominant $\nu_\mu \to \nu_\tau$ and $\bar{\nu}_\mu \to \bar{\nu}_\tau$ transitions of the atmospheric ν_μ or $\bar{\nu}_\mu$. In the case of $3-\nu$ mixing one can choose $\Delta m^2_{\rm atm} = \Delta m^2_{31}$, and Δm^2_{31} will be positive or negative depending on whether the neutrino mass spectrum is hierarchical, i.e., $m_1 < m_2 < (\ll) m_3$, $m_{1,2,3}$ being the neutrino masses, or is with inverted hierarchy, i.e., $m_3 (\ll) < m_1 \cong m_2$ [c]. Which of the two transitions $\nu_e \to \nu_\mu$ and $\bar{\nu}_e \to \bar{\nu}_\mu$ will be suppressed or resonantly enhanced by the Earth matter effect depends on the sign of $\Delta m^2_{31} \cos 2\theta_{13}$ (see further). The CHOOZ [12], solar and atmospheric neutrino data imply $\tan^2 \theta_{13} < 0.09$ [6]. Consequently, we have $\cos 2\theta_{13} > 0$ and if $\Delta m^2_{31} > 0$, the $\nu_e \to \nu_\mu$ transitions will be matter-enhanced while the transitions $\bar{\nu}_e \to \bar{\nu}_\mu$ will be suppressed, and *vice versa* for $\Delta m^2_{31} < 0$. Resolving this ambiguity is extremely important for, e.g., understanding the neutrino mass spectrum, for the predictions of the effective Majorana mass in neutrinoless double beta decay in the case the massive neutrinos are Majorana particles [11,13], etc. The resonance amplification of the $\nu_\mu \to \nu_e$ ($\nu_e \to \nu_\mu$) or $\bar{\nu}_\mu \to \bar{\nu}_e$ ($\bar{\nu}_e \to \bar{\nu}_\mu$) transitions and the suppression of the corresponding antineutrino or neutrino transitions by the Earth matter effects provides an opportunity to get information about the Earth density distribution along the neutrino trajectory in the Earth as well (see, e.g., [14]).

The matter effects in neutrino oscillations can play very important role in astrophysics (supernovae dynamics, etc.) and cosmology (see, e.g., [15]).

It should be clear from the preceding discussion that the matter effects in neutrino oscillations will play a significant role in the interpretation of the results of a neutrino factory experiment using a $L \gtrsim 1000$ km baseline, at which they are significant (see further). They will be crucial, in particular, for the searches for CP-violation in such experiments [16,17,18,19,3,20,14,21,22,23], since matter effects generate an asymmetry between the two relevant CP-conjugated appearance neutrino oscillation channels. Knowing the asymmetry caused by matter effects is therefore essential for obtaining information on the CP-violation originating from the lepton mixing matrix.

Calculating the oscillation probabilities and event rates for different channels and

[c] One can always numerate the three massive neutrinos in such a way that $m_1 < m_2 < m_3$. The spectrum with inverted hierarchy will correspond then to $m_1 < (\ll) m_2 \cong m_3$. However, in this case one has also to redefine the mixing angles responsible for the solar and atmospheric neutrino oscillations in terms of the elements of the neutrino mixing matrix (see, e.g., [11]).

comparing with those for oscillations in vacuum we have found [3] that the asymmetry between the $\nu_e \leftrightarrow \nu_\mu$ and $\bar{\nu}_e \leftrightarrow \bar{\nu}_\mu$ oscillations is the most promising tool to test and verify the MSW effect. The reason is that matter effects lead to measurably enhanced event rates in one of the two channels and to suppressed transitions in the other. The asymmetry between the event rates associated with these two channels would therefore be very sensitive to the MSW effect since the matter induced changes have opposite effect on the two rates thus amplifying the "signal". In [3] we have analyzed event rates and included statistical aspects, so that the results can be directly applied for the planning of optimal experimental setups.

Neutrino factories are extensively discussed in the literature, see, e.g., [4,21,22,23,24] and the references quoted therein. Either μ^- or μ^+ are accelerated to an energy E_μ and decay then in straight sections of a storage ring like $\mu^- \to e^- + \bar{\nu}_e + \nu_\mu$ or $\mu^+ \to e^+ + \bar{\nu}_\mu + \nu_e$, so that a very pure neutrino beam containing $\bar{\nu}_e$ and ν_μ or ν_e and $\bar{\nu}_\mu$, respectively, is produced. The muon energy E_μ could be in a wide range from 10 GeV to 50 GeV or more and a neutrino flux corresponding to $2 \cdot 10^{20}$ muon decays per year in the straight section of the ring pointing to a remote detector could be achieved. Higher fluxes are also currently under discussion (see, e.g., [24]). The neutrino fluxes are therefore very intense and can be easily calculated from the decay spectrum at rest. For unpolarized muons and negligible beam divergence one finds for a baseline of $L = 3000$ km ($L = 7000$ km) a neutrino flux of $\sim 2.5 \cdot 10^{11}$ ($5.1 \cdot 10^{10}$) $\mathrm{yr}^{-1}\mathrm{m}^{-2}$. The $\bar{\nu}_e$ and ν_e fluxes depend on the muon beam polarization, which will be assumed to be negligible in this paper. Altogether a neutrino factory would provide pure and high-intensity neutrino beams with a well known energy spectrum that in turn would allow a wide physical program including precise measurement of mixing parameters, matter effects and, in case of LMA solution of the solar problem - leptonic CP-violation.

The produced neutrino beam will be directed towards a remote detector at a given Nadir angle h, which corresponds to an oscillation baseline $L = 2R_\oplus \cos(h)$, where $R_\oplus = 6371$ km is the Earth radius. If $L \gtrsim 10^3$ km, as we shall assume, matter effects are important in neutrino oscillations. For $L \leq 10660$ km the beam traverses the Earth along a trajectory in the Earth mantle without crossing the Earth core where the density is substantially higher. According to the Earth models [25], the average matter density along the neutrino trajectories with $L = (10^3 - 10^4)$ km lies in the interval $\sim$ (2.9 - 4.8) $\mathrm{g/cm}^3$. The matter density changes along each trajectory, but the variation is relatively small - by about 1.5 to 2.0 $\mathrm{g/cm}^3$, and even the largest takes place over relatively big distances of several thousand kilometers. As a consequence, one can approximate the Earth mantle density profile by a constant average density distribution. The constant density should be chosen to be equal to the average density along every trajectory [26,9]. For the calculation of the neutrino oscillation probabilities of interest, the indicated constant density model provides a very good approximation to the somewhat more complicated density structure of the Earth mantle [26,9,27]. Let us note also that the Earth mantle is with a good precision isotopically symmetric:

$Y_e = 0.494$ [28], where Y_e is the electron fraction number in the mantle.

Since the beam consists always either of ν_e together with $\bar{\nu}_\mu$ or $\bar{\nu}_e$ in combination with ν_μ, there are, in principle, eight different appearance experiments and four different disappearance experiments which could be performed. From an experimental point of view, however, at present the four channels with muon neutrinos or antineutrinos in the final state, $\nu_\mu \to \nu_\mu$, $\bar{\nu}_\mu \to \bar{\nu}_\mu$, $\nu_e \to \nu_\mu$, $\bar{\nu}_e \to \bar{\nu}_\mu$ seem to be most promising. A very important issue is in this context the ability of the detector to discriminate between neutrinos and antineutrinos, namely the ability to measure the charge of the leptons produced by the neutrino charged current interactions. Very good discrimination capability is required for a measurement of the appearance probabilities since they produce "wrong sign" muon events in the detector and have to be discriminated from the much larger number of events associated with the ν_μ and $\bar{\nu}_\mu$ survival probabilities. The channels with ν_e or $\bar{\nu}_e$ in the final state are problematic from this point of view due to the difficulty of distinguishing e^+ from e^- in a large high-density detector. On the contrary, a very good μ^+/μ^- discrimination could be obtained in a large properly oriented magnetized detector [29].

2. Probabilities of Three-Neutrino Oscillations in Matter

We will assume three flavour neutrino mixing:

$$|\nu_l > \ = \sum_{k=1}^{3} U_{lk} |\nu_k > \ , \qquad l = e, \mu, \tau, \tag{1}$$

$|\nu_l >$ is the state vector of the (left-handed) flavour neutrino ν_l, $|\nu_k >$ is the state vector of a neutrino ν_k having a definite mass m_k, $m_k \neq m_j$, $k \neq j = 1, 2, 3$ and U is a 3×3 unitary matrix – the Pontecorvo-Maki-Nakagawa-Sakata (PMNS) neutrino mixing matrix. In this analysis we use a standard parametrization of U:

$$\begin{pmatrix} U_{e1} & U_{e2} & U_{e3} \\ U_{\mu 1} & U_{\mu 2} & U_{\mu 3} \\ U_{\tau 1} & U_{\tau 2} & U_{\tau 3} \end{pmatrix} = \begin{pmatrix} c_{12}c_{13} & s_{12}c_{13} & s_{13}e^{-i\delta} \\ -s_{12}c_{23} - c_{12}s_{23}s_{13}e^{i\delta} & c_{12}c_{23} - s_{12}s_{23}s_{13}e^{i\delta} & s_{23}c_{13} \\ s_{12}s_{23} - c_{12}c_{23}s_{13}e^{i\delta} & -c_{12}s_{23} - s_{12}c_{23}s_{13}e^{i\delta} & c_{23}c_{13} \end{pmatrix} \tag{2}$$

Here $c_{ij} \equiv \cos\theta_{ij}$, $s_{ij} \equiv \sin\theta_{ij}$, δ is the Dirac CP-violation phase, and $0 \leq \theta_{12}, \theta_{23}, \theta_{13} < \pi/2$, $0 \leq \delta < 2\pi$. We conventionally order the masses in such a way that

$$0 < \Delta m^2_{21} < |\Delta m^2_{31}|. \tag{3}$$

This includes the cases of neutrino mass spectrum with normal hierarchy

$$\Delta m^2_{31} > 0 : \qquad m_3 > m_2 > m_1, \tag{4}$$

and with inverted hierarchy,

$$\Delta m^2_{31} < 0 : \qquad m_2 > m_1 > m_3, \tag{5}$$

As long as matter and CP-violation effects are not taken into account, the two cases of neutrino mass spectrum - with normal and with inverted hierarchy, are phenomenologically equivalent from the point of view of neutrino oscillations.

It is natural to suppose that the neutrino mass-squared difference responsible for solar neutrino oscillations $\Delta m^2_{\odot} = \Delta m^2_{21}$. The different solutions of the solar neutrino problem correspond to [5,6,7]:

$$\text{LMA MSW} \quad : \quad 2.0 \times 10^{-5}\ \text{eV}^{\ 2} \lesssim \Delta m^2_{21} \lesssim 8.0 \times 10^{-4}\ \text{eV}^{\ 2}\ , \tag{6}$$

$$\text{SMA MSW} \quad : \quad 4.0 \times 10^{-6}\ \text{eV}^{\ 2} \lesssim \Delta m^2_{21} \lesssim 9.0 \times 10^{-6}\ \text{eV}^{\ 2}\ , \tag{7}$$

$$\text{LOW} - \text{QVO} \quad : \quad 5.0 \times 10^{-10}\ \text{eV}^{\ 2} \lesssim \Delta m^2_{21} \lesssim 2.0 \times 10^{-7}\ \text{eV}^{\ 2}\ . \tag{8}$$

The neutrino mass-squared difference and mixing angle controlling the dominant $\nu_\mu \leftrightarrow \nu_\tau$ and $\bar{\nu}_\mu \leftrightarrow \bar{\nu}_\tau$ oscillations of the atmospheric ν_μ or $\bar{\nu}_\mu$, are then $\Delta m^2_{\text{atm}} = \Delta m^2_{31}$ and θ_{23}. From the analysis of the atmospheric neutrino data one finds [8,7]

$$1.2 \times 10^{-3}\ \text{eV}^{\ 2} \lesssim |\Delta m^2_{31}| \lesssim 6.8 \times 10^{-2}\ \text{eV}^{\ 2} \qquad (99\%\ C.L.), \tag{9}$$

and $0.85 \lesssim \sin^2 2\theta_{23} \leq 1$.

For $E_\nu \geq 1\,\text{GeV}$ $(1\,\text{MeV})$, $L \leq 10^4$ (10) km and $\Delta m^2_{21} \lesssim 10^{-4}\,\text{eV}^{\ 2}$ (so that $\Delta m^2_{21} \ll |\Delta m^2_{31}|$), the probabilities of 3-ν oscillations in vacuum reduce effectively to 2-ν vacuum oscillation probabilities [30,31]:

$$P^{3\nu}_{vac}(\nu_l \to \nu_{l'}) = P^{vac}(\bar{\nu}_l \to \bar{\nu}_{l'}) \cong 2|U_{l3}|^2|U_{l'3}|^2 \left(1 - \cos\frac{\Delta m^2_{31}L}{2E}\right)\ ,\ l \neq l', \tag{10}$$

$$P^{3\nu}_{vac}(\nu_l \to \nu_l) = P^{3\nu}_{vac}(\bar{\nu}_l \to \bar{\nu}_l) \cong 1 - 2|U_{l3}|^2(1 - |U_{l3}|^2) \left(1 - \cos\frac{\Delta m^2_{31}L}{2E}\right), \tag{11}$$

where $l, l' = e, \mu, \tau$. Under the indicated conditions the element $|U_{e3}| = s_{13}$ of the lepton mixing matrix, which controls the $\nu_e \leftrightarrow \nu_{\mu(\tau)}$, $\bar{\nu}_e \leftrightarrow \bar{\nu}_{\mu(\tau)}$, $\nu_\mu \leftrightarrow \nu_e$ and the $\bar{\nu}_\mu \leftrightarrow \bar{\nu}_e$ oscillations, is constrained by the data from the CHOOZ and Palo Verde experiments [12,32] and the oscillation interpretation of the solar and atmospheric neutrino data [6]:

$$|\Delta m^2_{31}| \geq 1.5 \times 10^{-3}\ \text{eV}^{\ 2}: \qquad |U_{e3}|^2 \lesssim 0.09 \quad (99\%\ \text{C.L.}). \tag{12}$$

The precise upper limit in eq. (12) is $|\Delta m^2_{31}|$–dependent [12,6]. For $\Delta m^2_{21} \lesssim 10^{-4}\ \text{eV}^{\ 2}$ it does not depend, however, on the sign of Δm^2_{31}.

For $|\Delta m^2_{31}| \gtrsim 1.0 \times 10^{-3}\ \text{eV}^{\ 2}$ and $\Delta m^2_{21} \ll |\Delta m^2_{31}|$, the probability of solar ν_e survival when the solar ν_e travel from the central region of the Sun to the surface of the Earth (without crossing the Earth) reads [33] (see also, e.g., [34])

$$P^{3\nu}_{MSW,VO}(\nu^{\odot}_e \to \nu^{\odot}_e) \cong |U_{e3}|^4 + (1 - |U_{e3}|^2)^2\ P^{2\nu}_{MSW,VO}(\nu^{\odot}_e \to \nu^{\odot}_e; \Delta m^2_{21}, \theta_{12}, \theta_{13}), \tag{13}$$

where $P^{2\nu}_{MSW,VO}(\nu_e^\odot \to \nu_e^\odot; \Delta m^2_{21}, \theta_{12}, \theta_{13})$ is the well-known two-neutrino mixing MSW (see, e.g., [35,36]) or (quasi-) vacuum oscillation (see, e.g., [31,35,37]) probability, and

$$\sin^2 2\theta_{12} = 4\frac{|U_{e1}|^2\ |U_{e2}|^2}{(1-|U_{e3}|^2)^2}, \quad \cos 2\theta_{12} = \frac{|U_{e1}|^2 - |U_{e2}|^2}{1-|U_{e3}|^2}\ . \tag{14}$$

For $|U_{e3}|^2$ satisfying the CHOOZ limit, the dependence of $P^{3\nu}_{MSW,VO}(\nu_e^\odot \to \nu_e^\odot)$ on $|U_{e3}|^2$ is rather weak and cannot be used to further constrain or determine $|U_{e3}|^2$.

If $\Delta m^2_{21} \lesssim 10^{-4}$ eV $^2 \ll |\Delta m^2_{31}|$, the solar neutrino survival probability depends only on the absolute values of the elements of the first row of the lepton mixing matrix, i.e., on $|U_{ei}|^2$, i=1,2,3, while the oscillations of the (atmospheric) ν_μ, $\bar\nu_\mu$, ν_e and $\bar\nu_e$ on Earth distances are controlled by the elements of the third column of U, $|U_{l3}|^2$, $l = e, \mu, \tau$. The other elements of U are not accessible to direct experimental determination in solar and atmospheric neutrino and long baseline terrestrial experiments.

For $\Delta m^2_{21} \lesssim 5 \cdot 10^{-5}$ eV $^2 \ll |\Delta m^2_{31}|$ and in constant density approximation, one has for the probabilities of neutrino transitions in the Earth mantle [33,38] (see also, e.g., [39]):

$$P^{3\nu}_E(\nu_\mu \to \nu_e) = P^{3\nu}_E(\nu_e \to \nu_\mu) \cong s^2_{23} P^{2\nu}_E(\Delta m^2_{31}, \sin^2 2\theta_{13})\ , \tag{15}$$

$$P^{3\nu}_E(\nu_\mu \to \nu_\mu) \cong c^4_{23} + s^4_{23}\left[1 - P^{2\nu}_E(\Delta m^2_{31}, \sin^2 2\theta_{13})\right]$$

$$+\ 2c^2_{23}s^2_{23}\ \left[\cos\kappa - (1+\cos 2\theta^m_{13})\ \sin\frac{\Delta E_m L}{2}\ \sin(\kappa + \frac{\Delta E_m L}{2})\right]\ , \tag{16}$$

$$P^{3\nu}_E(\nu_\mu \to \nu_\tau) \cong\ 2c^2_{23}s^2_{23}\ \left[2\sin^2\frac{\kappa}{2} - \frac{1}{2}P^{2\nu}_E(\Delta m^2_{31}, \sin^2 2\theta_{13})\right.$$

$$\left. +\ (1+\cos 2\theta^m_{13})\ \sin\frac{\Delta E_m L}{2}\ \sin(\kappa + \frac{\Delta E_m L}{2})\right]\ , \tag{17}$$

where

$$P^{2\nu}_E(\Delta m^2_{31}, \sin^2 2\theta_{13}) = \frac{1}{2}\left[1 - \cos\Delta E_m L\right]\sin^2 2\theta^m_{13} \tag{18}$$

is the 2-ν transition probability in matter with constant density,

$$\kappa \cong \frac{L}{2}\ \left[\frac{\Delta m^2_{31}}{2E} + V - \Delta E_m\right] \tag{19}$$

is a phase, ΔE_m and θ^m_{13} are the neutrino energy difference and mixing angle in matter,

$$\Delta E_m = \frac{|\Delta m^2_{31}|}{2E}C_+, \quad \cos 2\theta^m_{13} = \frac{1}{C_+}\left(\cos 2\theta_{13} - \frac{2EV}{\Delta m^2_{31}}\right)\ , \tag{20}$$

where

$$C^2_\pm = \left(1 \mp \frac{2EV}{\Delta m^2_{31}}\right)^2 \pm 4\frac{2EV}{\Delta m^2_{31}}\sin^2\theta_{13} \tag{21}$$

and

$$V = \sqrt{2} G_F \bar{N}_e^{man} \tag{22}$$

is the matter term, $\bar{N}_e^{man}$ being the average electron number density along the neutrino trajectory in the Earth mantle. The probability $P_E^{3\nu}(\nu_e \to \nu_\tau)$ can be obtained from eq. (15) by replacing the factor s_{23}^2 with c_{23}^2. The corresponding antineutrino transition and survival probabilities have the same form and can formally be obtained from eqs. (15–17) by changing the sign of the matter term, i.e. $\bar{N}_e^{man} \to -\bar{N}_e^{man}$ in the expressions for κ, ΔE_m, $\cos 2\theta_{13}^m$, eqs. (19)–(20), and by replacing C_+ by C_-.

At distances $L \lesssim 7000$ km and for $\Delta m_{21}^2 \gtrsim 5 \cdot 10^{-5}$ eV^2, the Δm_{21}^2 corrections in $P_E^{3\nu}(\nu_\mu \to \nu_e)$, $P_E^{3\nu}(\nu_\mu \to \nu_\mu)$ and $P_E^{3\nu}(\nu_\mu \to \nu_\tau)$ can be non-negligible. It is possible to derive also the expressions for these probabilities including the leading order (CP-conserving and CP-violating) Δm_{21}^2-corrections by using the results of [33]. One finds in the case of $P_E^{3\nu}(\nu_e \to \nu_\mu)$ [3] (see also [20,40]):

$$P_E^{3\nu}(\nu_e \to \nu_\mu) \cong s_{23}^2 \, [1 + \cos\delta \cot\theta_{23} \sin 2\theta'_{23}] \, P_E^{2\nu}(\, \overline{\Delta m}^2_{31}, \theta_{13}) + \cos\theta'_{12} \, \sin 2\theta_{23} \, \sin 2\bar{\theta}^m_{13}$$
$$\times \, \sin\frac{\Delta \bar{E}_m L}{2} \left[\cos\delta \left(\sin(\bar{\kappa} + \frac{\Delta \bar{E}_m L}{2}) \right.\right.$$
$$\left.\left. - \, \cos 2\bar{\theta}^m_{13} \sin\frac{\Delta \bar{E}_m L}{2} \right) \, - 2 \sin\delta \, \sin\frac{\bar{\kappa}}{2} \, \sin(\frac{\bar{\kappa}}{2} + \frac{\Delta \bar{E}_m L}{2}) \right] \, , \tag{23}$$

where

$$\overline{\Delta m}^2_{31} \equiv \Delta m_{31}^2 - s_{12}^2 \Delta m_{21}^2 \, , \tag{24}$$

$$\bar{\kappa} = \frac{L}{2} \, \left[\frac{\overline{\Delta m}^2_{31}}{2E} + V - \Delta \bar{E}_m \right] - \frac{L \Delta m_{21}^2}{2E} \cos 2\theta_{12} \tag{25}$$

and

$$\cos\theta'_{12} = \frac{\Delta m_{21}^2 c_{12} s_{12} c_{13}}{2EV + s_{13}^2 \, \overline{\Delta m}^2_{31} - \Delta m_{21}^2 \cos 2\theta_{12}} \cong \frac{\Delta m_{21}^2 c_{12} s_{12} c_{13}}{2EV + s_{13}^2 \, \Delta m_{31}^2} \, , \tag{26}$$

$$\sin 2\theta'_{23} = - \, \frac{\Delta m_{21}^2 s_{13} \sin 2\theta_{12}}{\overline{\Delta m}^2_{31} c_{13}^2 - \Delta m_{21}^2 \cos 2\theta_{12}} \cong - \, \frac{\Delta m_{21}^2}{\Delta m_{31}^2} \, s_{13} \sin 2\theta_{12} \, . \tag{27}$$

The expressions for $P_E^{2\nu}(\, \overline{\Delta m}^2_{31}, \theta_{13})$, $\Delta \bar{E}_m$ and $\cos 2\bar{\theta}^m_{13}$ are given by (18) and (20) in which $\Delta m_{31}^2 \to \overline{\Delta m}^2_{31}$, while $P_E^{3\nu}(\bar{\nu}_e \to \bar{\nu}_\mu)$ ($P_E^{3\nu}(\nu_\mu \to \nu_e)$) can formally be obtain from eq. (23) by making the changes $V \to -V$ and $\delta \to -\delta$ ($\delta \to -\delta$). The terms $\sim \cos\delta$ and $\sim \sin\delta$ in eq. (23) include the leading order CP-conserving and CP-violating Δm_{21}^2−corrections, associated with the phase δ.

The expression (23) is derived by neglecting terms $\sim (\cos\theta'_{12})^2$, $(\sin 2\theta'_{23})^2$, $\cos\theta'_{12} \times$ $\times \sin 2\theta'_{23}$ and higher order corrections. For $L \geq 1000$ km of interest, eq. (23) describes the probability $P_E^{3\nu}(\nu_e \to \nu_\mu)$ with a sufficiently high precision for $\Delta m_{21}^2 \lesssim 2 \times 10^{-4}$ eV^2 and $E \gtrsim 4.5$ GeV. If $|\Delta m_{31}^2| \cong 3.5 \times 10^{-3}$ eV^2, the correction $\sim \cos\theta'_{12}$ would be the dominant one for $E \sim (5 - 30)$ GeV.

Few comments are in order. The analytic expressions eqs. (15)–(17) represent excellent approximations in the case of the LOW-QVO and SMA MSW solutions of the solar neutrino problem and for values of $\Delta m^2_{21} \lesssim 5 \times 10^{-5}$ eV ^{2} from the LMA solution region. For 5×10^{-5} eV $^2 < \Delta m^2_{21} \lesssim$ few $\times 10^{-4}$ eV ^{2}, the corrections due to Δm^2_{21} can be nonnegligible. Further, $P^{3\nu}_E(\nu_e \to \nu_\mu)$ and $P^{3\nu}_E(\bar\nu_e \to \bar\nu_\mu)$ cannot exceed $s^2_{23} \sim 0.5$. The maximum value $\max(P^{3\nu}_E(\nu_e \to \nu_\mu)) = s^2_{23}$, is reached only if $\sin^2 2\theta^m_{13} = 1$ and $\cos \Delta E_m L = -1$. At the MSW resonance one has $\Delta E^{res}_m \cong 1.23\pi \times 10^{-4}$ km^{-1} $\tan 2\theta_{13} \bar N^{man}_e [N_A \mathrm{cm}^{-3}]$. For $s^2_{13} \leq 0.025$, $\cos \Delta E^{res}_m L = -1$ can only be satisfied for $L \geq 10^4$ km. If $s^2_{13} = 0.05$, $\cos \Delta E^{res}_m L = -1$ requires $L \geq 8 \times 10^3$ km.

The MSW resonance energy is given by $E_{\rm res} \cong 6.56 \times \Delta m^2_{31}[10^{-3}\ \mathrm{eV}^{\,2}] \cos 2\theta_{13} \times$ $\times (\bar N^{man}_e [cm^{-3} N_A])^{-1}$ GeV, where Δm^2_{31} is in units of 10^{-3} eV ^{2}. For $\Delta m^2_{31}[10^{-3}\ \mathrm{eV}^{\,2}]$ $= 2.5; 3.5; 6.5$, and, e.g., $\bar N^{man}_e [cm^{-3} N_A] = 2$, we have $E_{\rm res}[\,\mathrm{GeV}] \cong 8.2; 11.5; 21.3 \times$ $\times \cos 2\theta_{13}$. The $\nu_e \to \nu_\mu$ and $\bar\nu_e \to \bar\nu_\mu$ oscillations will be affected substantially by the MSW effect if the energy of the parent muon beam $E_\mu > E_{\rm res}$. This condition can be satisfied for any value of Δm^2_{31} from the interval (9) for $E_\mu \gtrsim 23\,\mathrm{GeV}$. For the value of $\Delta m^2_{31}[10^{-3}\ \mathrm{eV}^{\,2}] = 2.5$ which is currently "favored" by the Super- Kamiokande data [8] we have $E_\mu \gtrsim 11\,\mathrm{GeV}$. Given the fact that the maxima of the spectra of ν_e and $\bar\nu_e$ from $\mu^\pm-$decays occur at $E = 2E_\mu/3$, the muon energy should not be much larger than the resonance energy since in the opposite case only a relatively small fraction of the neutrinos from the ν_e and $\bar\nu_e$ fluxes will undergo transitions which will be affected by the matter effects.

Finally, a change in the sign of Δm^2_{31} reverses the sign of N^{res}_e which opens the possibility to determine the sign of Δm^2_{31} via matter effects [10,3].

3. Matter Effects in the Event Rates

We will discuss in this Section the effects of matter on the total rates of $\nu_e \to \nu_\mu$, $\bar\nu_e \to \bar\nu_\mu$, $\nu_\mu \to \nu_\mu$, $\bar\nu_\mu \to \bar\nu_\mu$ events. The $\nu_e \to \nu_\mu$ oscillations of the ν_e originating in the μ^+-decays of the μ^+ accumulated in the storage ring of a neutrino factory, will produce μ^--events, or "wrong sign" muon events in the detector, in addition to the standard μ^+-events. We will denote the corresponding "wrong sign" and standard muon event rates as $n_{\mu^+}(\mu^-)$ and $n_{\mu^+}(\mu^+)$, respectively. Likewise, the $\bar\nu_e \to \bar\nu_\mu$ oscillations of the $\bar\nu_e$ from the μ^--decays of a μ^--beam will generate "wrong sign", i.e., μ^+-events, in the detector together with the standard μ^-- events. The respective event rates will be denoted as $n_{\mu^-}(\mu^+)$ and $n_{\mu^-}(\mu^-)$.

We present quantitative results for the indicated total event rates for $\Delta m^2_{21} \ll 10^{-4}$ eV ^{2} in the case of oscillations in the Earth mantle and compare them with the results one would obtain if the oscillations took place in vacuum. The total event rates depend in a transparent way (see [3]) on the following experimental parameters: i) the number of "useful" $\mu^\pm-$ decays, occurring in the straight section of the storage ring pointing to the detector, $N_{\mu^\pm}$, ii) the size of the detector in kilotons, $N_{\rm kT}$ iii) the

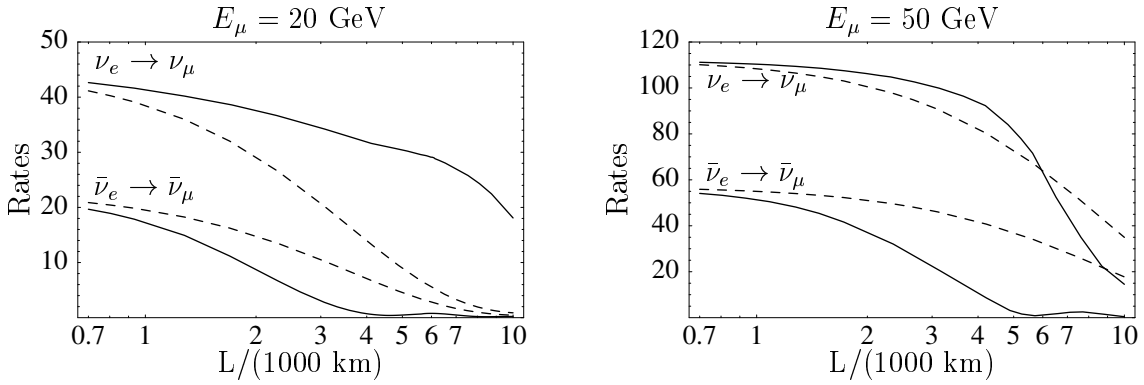

Figure 1: Appearance event rates $n_{\mu^+}(\mu^-)$, $n_{\mu^-}(\mu^+)$ due to the $\nu_e \to \nu_\mu$ and $\bar{\nu}_e \to \bar{\nu}_\mu$ transitions in the Earth mantle (solid lines) and in vacuum (dashed lines), as functions of the baseline L for $E_\mu = 20\,\mathrm{GeV}$ (left) and $E_\mu = 50\,\mathrm{GeV}$ (right). The differences between the solid and dashed lines is a measure of the magnitude of the Earth matter effect. Both plots are obtained for $N_\mu = 2 \cdot 10^{20}$, $\epsilon = 50\%$, $\sin^2 2\theta_{23} = 1$, $\sin^2 2\theta_{13} = 0.01$, $\Delta m^2_{31} = 3.5 \cdot 10^{-3}$ eV ^{2} and $\Delta m^2_{21} \ll 10^{-4}$ eV ^{2}. The scaling of the rates with these parameters is described in [1)].

energy of the muons in the ring [d], E_μ, and vi) the $\mu^\pm$ detection efficiencies, $\epsilon_{\mu^\pm}$. They depend also in a known way on the mixing parameters θ_{23}, θ_{13} and on the value and sign of Δm^2_{31}. We focus our discussion on the dependence on the baseline L and muon energy E_μ, using the standard value of $\Delta m^2_{31} = 3.5 \cdot 10^{-3}$ eV ^{2} and assuming that $\Delta m^2_{31} > 0$. For $\Delta m^2_{21} \ll 10^{-4}$ eV ^{2}, the CP-violation effects are negligible and the results for $\Delta m^2_{31} < 0$ can be obtained by simply interchanging neutrinos and antineutrinos. The contribution of the background to the number of muons observed in the detector, as well as the effects of a possible divergence of the muon beam in the straight section of the storage ring, are neglected in the present analysis [e].

The total number of events in the two appearance channels $\nu_e \to \nu_\mu$, $\bar{\nu}_e \to \bar{\nu}_\mu$ are shown for $E_\mu = 20\,\mathrm{GeV}$ and $E_\mu = 50\,\mathrm{GeV}$ in Fig. 1 as a function of the baseline (solid lines) in comparison with the event rates one would get if the neutrino oscillations took place in vacuum (dashed lines). In Fig. 2 we show the same results for the two disappearance channels $\nu_\mu \to \nu_\mu$, $\bar{\nu}_\mu \to \bar{\nu}_\mu$. Both figures correspond to a "default" experimental set-up providing $N_{\mu^+} = N_{\mu^-} = N_\mu = 2 \cdot 10^{20}$ useful muon decays (e.g. in one year of running) and to a detector with $N_{\mathrm{kT}} = 10$ kilotons and an efficiency $\epsilon_{\mu^+} = \epsilon_{\mu^-} = \epsilon = 50\%$ in both channels. The rates depend only on the combination $N_\mu N_{\mathrm{kT}} \epsilon$ which is in this case $N_\mu N_{\mathrm{kT}} \epsilon = 10^{21}$ [f].

[d] As a lower cut on the neutrino energies that can ensure a good detection efficiency we have used $E_{\mathrm{min}} = 3\,\mathrm{GeV}$, but the results do not depend significantly on the precise value of E_{min} for $E_{\mathrm{min}} < 5\,\mathrm{GeV}$.

[e] Studies indicated that the major sources of background in the experiments of interest can be kept under control in different ways [24,29,18)].

[f] The rates for different values of N_μ, N_{kT}, ϵ, θ_{23}, θ_{13} can be obtained by using eqs. (21a) - (21d) and (24a) - (24b) in [3)].

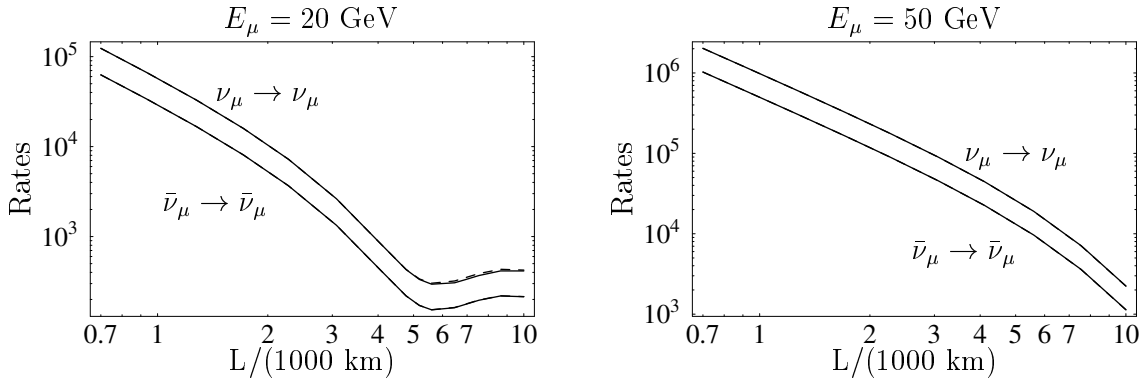

Figure 2: Same as in Fig. 1 but for the disappearance channels. The dashed lines almost coincide with the solid lines, showing that matter effects are rather small in these channels.

The vacuum event rates in the neutrino channels are twice as big as the rates in the antineutrino channels. This is because the oscillation probabilities are in the CP-conjugated channels in the $\Delta m^2_{21} \ll 10^{-4}$ eV ^{2} approximation the same, while the functions averaging the probabilities are larger by a factor 2 in the neutrino channels (due to the larger cross-section). The disappearance channels shown in Fig. 2 are essentially independent of matter effects since these effects come only with the θ_{13} corrections to the oscillation probabilities [g]. In contrast, Fig. 1 shows the drastic enhancement (depletion) of the event rates in the $\nu_e \to \nu_\mu$ ($\bar{\nu}_e \to \bar{\nu}_\mu$) channel for rather long baselines. The growth of the total rates with E_μ is clearly seen in Fig. 1.

Figures 3 and 4 show in more detail the differential event rates of the appearance channels $\nu_e \to \nu_\mu$ and $\bar{\nu}_e \to \bar{\nu}_\mu$ as three dimensional plots over L and E. The figures show clearly the enhancement (suppression) due to the Earth matter effects in the $\nu_e \to \nu_\mu$ ($\bar{\nu}_e \to \bar{\nu}_\mu$) channel for large baseline L. To understand these figures we consider the values of $dn_{\mu^+}(\mu^-)/dE$ and $dn_{\mu^-}(\mu^+)/dE$ for three different energies, $E = (5;\ 10;\ 15)\,\mathrm{GeV}$, and two baselines L: we compare results for a relatively short baseline $L = L_0 \equiv 1000$ km with those for a long baseline $L = 6000$ km, for which matter effects are more important. For $L = 1000$ km ($L = 6000$ km) the average matter electron density is $\bar{N}_e^{man} = 1.45\ \mathrm{cm}^{-3}\mathrm{N_A}$ ($\bar{N}_e^{man} \cong 2.0\ \mathrm{cm}^{-3}\mathrm{N_A}$), resulting in a resonance neutrino energy of $E_{res} = 15.8\,\mathrm{GeV}$ ($E_{res} = 11.5\,\mathrm{GeV}$). The corresponding values of $\Delta_{31}(L) \equiv L\ \Delta m^2_{31}/(4E)$ and the matter effect factors C_+ and C_-, which enter in $P^{3\nu}_E(\nu_e \to \nu_\mu)$ and $P^{3\nu}_E(\bar{\nu}_e \to \bar{\nu}_\mu)$ (see eqs. (15), (18), (20) and (21)), are displayed in Table 1. At 1000 km matter effects are small. C_+ (eq. 21) decreases as E changes from 5 to 15 GeV, approaching the resonance energy from below. Note that due to the matter term we have $C_+ < 1$ and $C_- > 1$ for the three values of E of interest. The argument of the oscillating sine factor in $P^{3\nu}_E(\nu_e \to \nu_\mu)$ and in

[g] As discussed in [3], effects as large as 20% can occur for θ_{13} close to the CHOOZ limit and relatively large baselines.

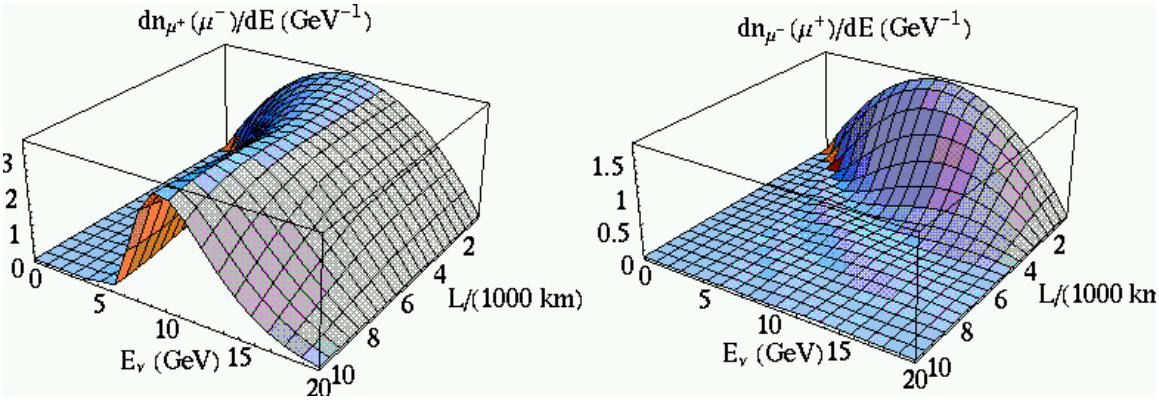

Figure 3: Differential appearance rates for the channels $\nu_e \to \nu_\mu$ (left) and $\bar{\nu}_e \to \bar{\nu}_\mu$ (right) as functions of L and E for the same values of the parameters for which Fig. 1 was obtained. The asymmetry, i.e., the enhancement of $dn_{\mu^+}(\mu^-)/dE$ and the suppression of $dn_{\mu^-}(\mu^+)/dE$, at $L \gtrsim (5000 - 6000)$ km is related to the MSW effect (see the text).

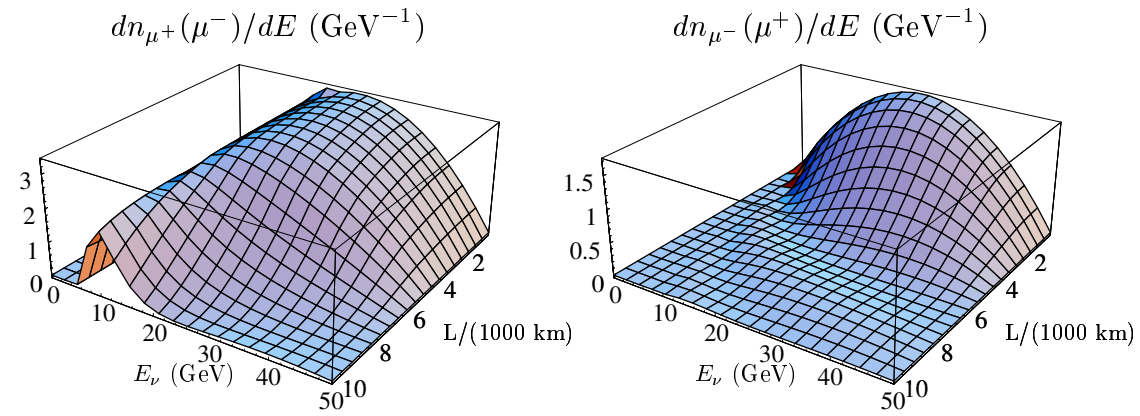

Figure 4: The same as in Fig. 3 but for a beam energy of 50 GeV.

$P^{3\nu}_E(\bar{\nu}_e \to \bar{\nu}_\mu)$ at values of E considered is relatively small, allowing an expansion of the sine in the oscillation probability $P^{3\nu}_E(\nu_e \to \nu_\mu) \cong s^2_{23} \sin^2(2\theta_{13})\ (\Delta_{31}(L_0))^2$. The fact that the matter effect factors cancel out reflects the negligibility of matter effects at short baselines. Neglecting matter effects at short baselines, the maximum of the differential event rate spectrum is at one half of the muon beam energy, which is 10 GeV in the case under discussion. At $L = 6000$ km, one has $\Phi(L) = \Phi(L_0)(L_0/L)^2 = \Phi(L_0)/36$, where $\Phi(L)$ is the flux of ν_e or $\bar{\nu}_e$ at distance $L \geq L_0$. The argument of the sine is large for the anti-neutrino channel giving for the corresponding rates the upper bound $dn_{\mu^-}(\mu^+)/dE \propto s^2_{23}\ g_{\bar{\nu}_e}(x)\ (\Phi(L_0)/36)\ (\sin^2 2\theta_{13}/C^2_-)\sin^2(\Delta_{31}(L)C_-) \leq s^2_{23}\ g_{\bar{\nu}_e}(x)\ (\Phi(L_0)/36)(\sin^2 2\theta_{13}/C^2_-)$, $g_{\bar{\nu}_e}(x)$ being the $\bar{\nu}_e$ spectrum and $x \equiv \mathrm{E}/\mathrm{E}_\mu$. Obviously, $dn_{\mu^-}(\mu^+)/dE$ is strongly suppressed primarily by the decreasing of the

L	1000km			6000km		
E	5 GeV	10 GeV	15 GeV	5 GeV	10 GeV	15 GeV
$\Delta_{31}(L)$	0.282π	0.141π	0.094π	1.694π	0.847π	0.565π
C_+	0.686	0.371	0.111	0.568	0.159	0.327
C_-	1.315	1.630	1.945	1.434	1.869	2.304
$\Delta_{31}(L)C_+$	0.610	0.167	0.031	3.023	0.424	0.580
$\Delta_{31}(L)C_-$	1.166	0.723	0.575	7.632	4.973	4.090

Table 1: Values of $\Delta_{31}(L) \equiv L\Delta m^2_{31}/(4E)$, C_+ and C_- for $\Delta m^2_{31} = 3.5 \times 10^{-3}$ eV ^{2}, $\sin^2 2\theta_{23} = 1$ and $\sin^2 2\theta_{13} = 0.01$ (see the text).

flux. The suppression due to the matter effect term $(1/{C_-}^2)$ for $E = (5 - 15)\,\mathrm{GeV}$ is by a factor of $\sim (2 - 5)$. The same conclusion is valid for $dn_{\mu^+}(\mu^-)/dE$ below the resonance region, say at $E = 5$ GeV. For neutrinos in the resonance region $E \cong (10 - 15)\,\mathrm{GeV}$, the argument of the sine is small even for very long baselines. As like in the case of short baselines, an expansion is possible: $dn_{\mu^+}(\mu^-)/dE \propto s^2_{23}\, g_{\nu_e}(x)\, \Phi(L_0)(L_0/L)^2\, (\sin^2 2\theta_{13}/C^2_+) \sin^2(\Delta_{31}(L)C_+) \cong s^2_{23}\, g_{\nu_e}(x)\, \Phi(L_0)\, \sin^2(2\theta_{13}) \times \times (\Delta m^2_{31} L_0/(4E))^2$. This is approximately equal to the same differential event rate at short baselines, e.g., at $L = 1000$ km. Thus, in the resonance region ($E \cong (10 - 15)\,\mathrm{GeV}$) and at sufficiently long baselines ($L \gtrsim 4000$ km), matter effects lead to a strong suppression of anti-neutrino event rate while keeping the neutrino event rate essentially constant with the change of L from ~ 1000 km to ~ 7000 km (see Fig. 3). In vacuum, however, the neutrino rate as well as the anti-neutrino rate would show the same strong $(L_0/L)^2$ suppression at long baselines.

For fixed $L \gtrsim 4500$ km, say at $L = 6000$ km, the matter effects lead to a strong enhancement of $dn_{\mu^+}(\mu^-)/dE$ as a function of E in a region which is somewhat wider than the MSW resonance region, $E \sim (8 - 15)$ GeV, in spite of the fact that in this region $\Delta_{31}(L)C_+ < 0.6$ and we have $dn_{\mu^+}(\mu^-)/dE \propto s^2_{23}\, g_{\nu_e}(x)\, \Phi(L) \times \times (\sin^2 2\theta_{13}/C^2_+) \sin^2(\Delta_{31}(L)C_+) \cong s^2_{23}\, g_{\nu_e}(x)\, \Phi(L)\, \sin^2 2\theta_{13}\, (\Delta_{31}(L))^2$. We have in the indicated energy region $\Delta_{31}(L) > 1$ and the enhancement of $dn_{\mu^+}(\mu^-)/dE$ compared to the case of $\nu_e \leftrightarrow \nu_\mu$ vacuum oscillations is actually given by the ratio of $(\Delta_{31}(L))^2$ and $\sin^2(\Delta_{31}(L))$.

4. Observing the Matter Effects, Determining the Sign of Δm^2_{31} and Measuring θ_{13}

We have seen that matter effects change the total event rates in the appearance channels $\nu_e \to \nu_\mu$ and $\bar{\nu}_e \to \bar{\nu}_\mu$ in very long baseline experiments in a drastic way. Such experiments would therefore offer unique possibilities to observe matter effects and to test the predictions of the MSW theory. A measurement of the shape of the neutrino energy spectrum, which is modified by the matter effects in a very characteristic way, would allow to test the detailed predictions of the theory. High differential event rates

and a good calibration of the detector would however be necessary for this option. We will discuss this possibility briefly in Section 6. Here we limit our discussion to the statistical significance of the matter effects in the total event rates and to the related problems of determining the sign of Δm^2_{31} and of measuring of, or deriving a stringent upper limit on, the value of $\sin^2 2\theta_{13}$.

Matter effects produce deviations of the total number of wrong sign muon events $n_{\mu^+}(\mu^-)$, $n_{\mu^-}(\mu^+)$ from what is expected in the absence of matter. These deviations occur in opposite directions in the two appearance channels. Suppose that a certain number of wrong sign muon events in the neutrino (antineutrino) appearance channel $n_{\mu^+}(\mu^-)$ ($n_{\mu^-}(\mu^+)$) is measured, while $\langle n^{\rm vac}_{\mu^+}(\mu^-)\rangle$ ($\langle n^{\rm vac}_{\mu^-}(\mu^+)\rangle$) would be expected in the absence of matter effects. We want to determine the confidence level at which $n_{\mu^+}(\mu^-)$ and $n_{\mu^-}(\mu^+)$ could represent statistical fluctuations around the expected values in vacuum $\langle n^{\rm vac}_{\mu^+}(\mu^-)\rangle$, $\langle n^{\rm vac}_{\mu^-}(\mu^+)\rangle$. Following the procedure proposed by the Particle Data Book [41], we calculate confidence levels by using [3]

$$\chi^2 = 2\left[\langle n^{\rm vac}_{\mu^+}(\mu^-)\rangle - n_{\mu^+}(\mu^-)\right] + 2n_{\mu^+}(\mu^-)\log\frac{n_{\mu^+}(\mu^-)}{\langle n^{\rm vac}_{\mu^+}(\mu^-)\rangle}$$

$$+2\left[\langle n^{\rm vac}_{\mu^-}(\mu^+)\rangle - n_{\mu^-}(\mu^+)\right] + 2n_{\mu^-}(\mu^+)\log\frac{n_{\mu^-}(\mu^+)}{\langle n^{\rm vac}_{\mu^-}(\mu^+)\rangle}. \qquad (28)$$

The corresponding "number of standard deviations" is given by $n_\sigma \equiv \sqrt{\chi^2}$. This prescription incorporates the available information in both the measured numbers $n_{\mu^+}(\mu^-)$, $n_{\mu^-}(\mu^+)$ in the most complete way. Note that the results thus obtained [3] depend on whether it is assumed that θ_{13} is known or that θ_{13} is only limited from above. In the latter case one should vary θ_{13} in the vacuum rates entering the definition of χ^2 in eq. (28) in the allowed range and find the minimum. This tends to reduce the significance at largest baselines.

The statistical method expressed by eq. (28) can be understood by defining the asymmetry

$$A := \frac{\Delta}{\Sigma} = \frac{n_{\mu^+}(\mu^-) - 2n_{\mu^-}(\mu^+)}{n_{\mu^+}(\mu^-) + 2n_{\mu^-}(\mu^+)} \qquad (29)$$

which, in particular, is very sensitive to effects which affect $n_{\mu^+}(\mu^-)$ and $n_{\mu^-}(\mu^+)$ in a opposite way. For small $\Sigma^{\rm vac}$ (i.e., relatively small beam energies), this method is related to comparing the absolute asymmetry expected in matter with the expected fluctuations of this quantity in the vacuum-case $\chi = \Delta/\delta\Delta^{\rm vac}$. For sufficiently large $\Sigma^{\rm vac}$ this is equivalent to doing the same with the asymmetry: $\chi = A/\delta A^{\rm vac}$.

As it is not difficult to convince oneself (see, e.g, [3]), the sign of the asymmetry A, or equivalently of Δ, is unambiguously related to the sign of Δm^2_{31}. Thus, the measurement of a non-zero value of the total event rate asymmetry A would allow to determine the sign of Δm^2_{31} and will provide information on the type of the neutrino mass spectrum (hierarchical or with inverted hierarchy) in the case of $3-\nu$ mixing.

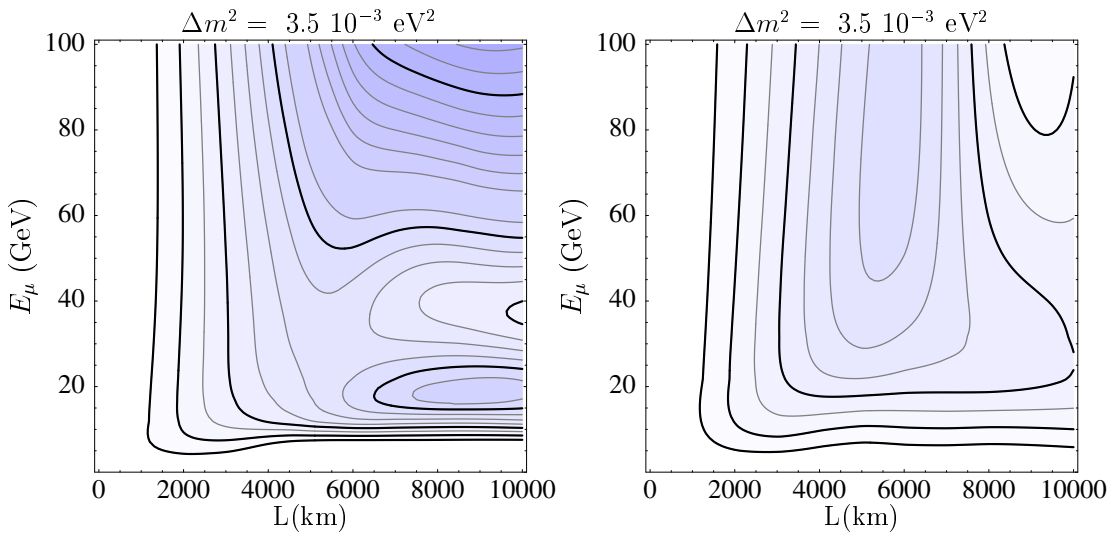

Figure 5: Contour lines of n_σ in the L-E_μ plane for $N_\mu N_{\rm kT}\epsilon = 10^{21}$. The solid contour lines correspond to $n_\sigma = 10 \sin 2\theta_{13} \cdot \{1, 2, 4, 8, 16\}$. The left plot was obtained assuming that θ_{13} is known, while the right plot was derived by varying θ_{13} in the range currently allowed.

Let us discuss next the dependence of n_σ on the relevant parameters. The dependence of n_σ on the intensity of the muon source and the detector size and efficiency, as well as the dependence on the mixing parameters is given by [3)]:

$$n_\sigma \propto (N_\mu N_{\rm kT} \epsilon_\mu)^{1/2} \ \text{ and } \ n_\sigma \propto \sin\theta_{23} \sin 2\theta_{13} \ . \tag{30}$$

The dependence of n_σ on the baseline L and the muon energy E_μ is less trivial. It is illustrated in Fig. 5 for $\Delta m^2_{31} = 3.5 \cdot 10^{-3}$ eV ^{2} and $N_\mu N_{\rm kT}\epsilon = 10^{21}$, where the contour lines of n_σ are plotted in the L-E_μ plane. The left plot assumes that θ_{13} is known, while the right plot was obtained by varying θ_{13} in the range currently allowed by the data. With the simple "total rates based" method described above and assuming that θ_{13} is known, any L from the interval $(4.0 - 10.0) \times 10^3$ km would be suitable for the purpose of detecting the matter effects if $\Delta m^2_{31} = 3.5 \times 10^{-3}$ eV ^{2}, $\sin^2 2\theta_{13} = 0.01$ and $E_\mu = 20$ GeV. At $E_\mu = 20$ GeV the sensitivity to matter effects is increasing with L up to $L \cong 7.0 \times 10^3$ km; for larger values of $L \leq 10 \times 10^3$ km it practically does not change. For $E_\mu = 50$ GeV, the sensitivity varies very little for $L \cong (5.0 - 10.0) \times 10^3$ km. If θ_{13} would not be known, the sensitivity of interest increases with the increasing of E_μ and L until the latter reach the values $E_\mu \cong 50$ GeV and $L \cong (6.0 - 7.0) \times 10^3$ km. Increasing further E_μ does not lead to a gain in sensitivity, while at $L \gtrsim 7.0 \times 10^3$ km the sensitivity actually becomes worse.

Let us note that at $L \gtrsim 3.0 \times 10^3$ km the matter effects are substantial for any neutrino energy E either in the $\nu_e \to \nu_\mu$ and/or in the $\bar\nu_e \to \bar\nu_\mu$ channel, depending on the sign of Δm^2_{31}: at $L \gtrsim 3.0 \times 10^3$ km we have $\sqrt{2} G_F \bar N_e^{man} L/2 \gtrsim 0.95$. The matter effects can be negligible for certain intervals of E for $L \lesssim 2.0 \times 10^3$ km.

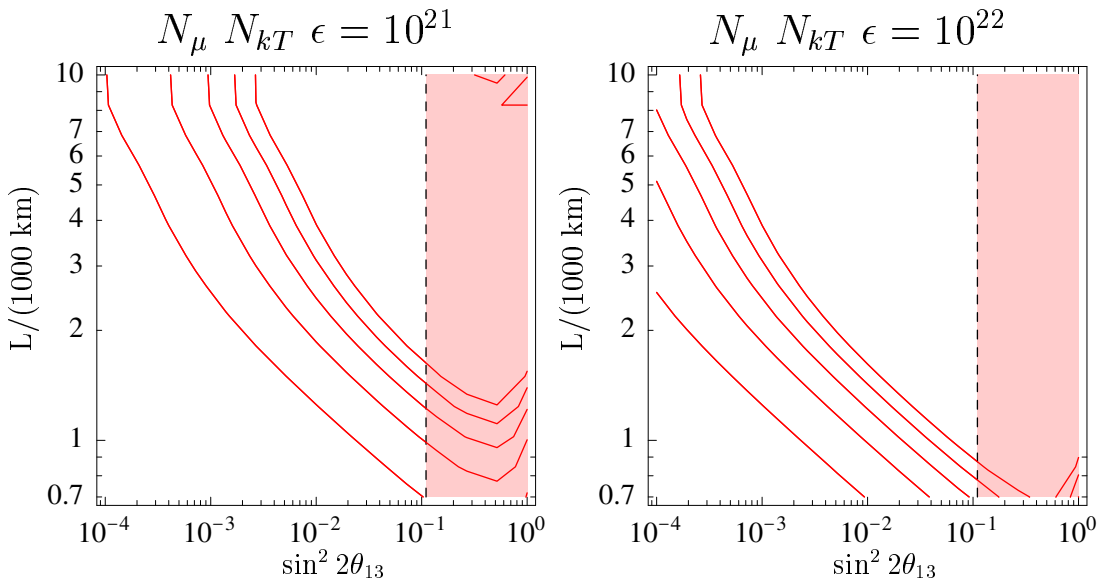

Figure 6: Contour lines of n_σ corresponding to $n_\sigma = 1, 2, 3, 4, 5$ in the $\sin^2 2\theta_{13}$-L plane for $E_\mu = 20\,\mathrm{GeV}$ and two different values $N_\mu N_{\mathrm{kT}}\epsilon$.

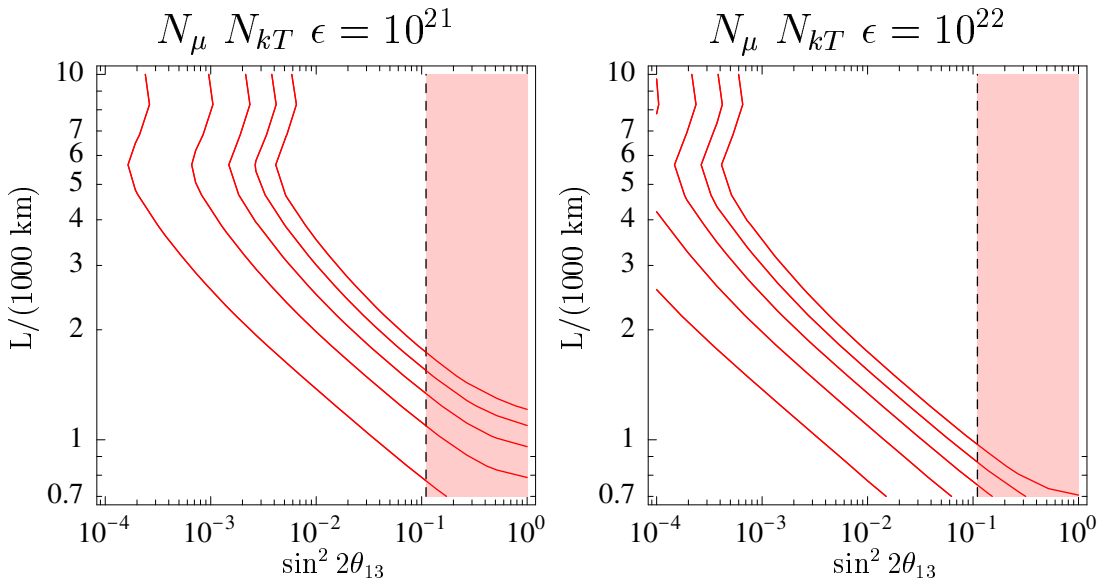

Figure 7: The same as in Fig. 6 but for $E_\mu = 50\,\mathrm{GeV}$.

At $L = 10^3$ km and for $\Delta m^2_{31} = 3.5 \times 10^{-3}$ eV ^{2}, $\sin^2 2\theta_{13} = 0.01$, for instance, the Earth matter effects cause a difference between $P^{3\nu}_E(\nu_e \to \nu_\mu)$, eq. (15), and the probability of the $\nu_e \to \nu_\mu$ transitions in vacuum $P^{3\nu}_{vac}(\nu_e \to \nu_\mu)$, eq. (10), which does

not exceed $\sim 5 \times 10^{-5}$ at $E \geq 10$ GeV. We have also $|P_E^{3\nu}(\bar{\nu}_e \to \bar{\nu}_\mu) - P_{vac}^{3\nu}(\bar{\nu}_e \to \bar{\nu}_\mu)| \leq 10^{-4}$ (10^{-5}) for $E \geq 10$ (20) GeV [h]. Thus, baselines $L \lesssim (2000 - 3000)$ km and parent muon energies $E_\mu \gtrsim (20 - 25)$ GeV seem to be better suited for searches of CP-violation in neutrino oscillations whose source is the lepton mixing matrix.

The significance of the matter effect, i.e., the number of standard deviations n_σ, depends most crucially on θ_{13} and L. We illustrate this dependence in Fig. 6 again for $\Delta m^2_{31} = 3.5 \cdot 10^{-3}$ eV ^{2}, where the contour lines corresponding to $n_\sigma = 1, 2, 3, 4, 5$ are plotted in the $\sin^2 2\theta_{13}$-L plane for two values of $N_\mu N_{\rm kT} \epsilon$: 10^{21} (left plot) and 10^{22} (right plot). The muon energy is in both cases $E_\mu = 20$ GeV. Results for $E_\mu = 50$ GeV and the same values of the other parameters are shown in Fig. 7. Figures 6 and 7 give an idea about the sensitivity of the discussed experiments to $\sin^2 2\theta_{13}$. The vertical dashed lines represent in both figures the upper limit on $\sin^2 2\theta_{13}$. Figures 6 and 7 show the $\sin^2 2\theta_{13}$ range where the enhancement/depletion of the total appearance rates in vacuum due to matter effects is statistically significant for a given confidence level. In those ranges one can not only observe the deviations from the results expected in vacuum, but also the deviation from the results which one would get in matter if the sign of Δm^2_{31} were reverted. A measurement of the sign of Δm^2_{31} would therefore be possible in the $\sin^2 2\theta_{13}$ range where matter effects are statistically significant [i]. Figures 6 - 7 indicate also that for baselines $L \cong (6 - 7) \times 10^3$ km, the discussed experiments will be sensitive to $\sin^2 2\theta_{13} \cong 10^{-3}$ even for $N_\mu N_{\rm kT} \epsilon = 10^{21}$.

5. Subleading CP-Violating and CP-Conserving Δm^2_{21}-Effects

The results discussed so far were obtained in the limit $\Delta m^2_{21} = 0$ which is a perfect approximation for $\Delta m^2_{21} \ll 10^{-4}$ eV ^{2} and/or $\sin^2 2\theta_{12} \ll 1$, i.e., for the LOW-QVO and SMA MSW solutions of the solar neutrino problem. In the case of the LMA MSW solution, however, $\sin^2 2\theta_{12} \sim (0.6 - 1.0)$ and, according to the recent global analyses of the solar and atmospheric neutrino and CHOOZ data [6,7], Δm^2_{21} can be as large as $(7.0 - 8.0) \cdot 10^{-4}$ eV ^{2}. Effects associated with Δm^2_{21} can be important, especially for $\Delta m^2_{21} \sim (1.0 - 8.0) \cdot 10^{-4}$ eV ^{2} in the LMA region.

If $\Delta m^2_{21} \gtrsim 5 \cdot 10^{-5}$ eV ^{2}, $\theta_{12} = \theta_\odot^{LMA}$ and δ become relevant [42,43], as the expression for $P_E^{3\nu}(\nu_e \to \nu_\mu)$, eq. (23), shows. While θ_{12} is rather tightly constrained by the solar neutrino data [6,7], any value of δ in its range $0 \leq \delta < 2\pi$ is allowed at present.

In Fig. 8 we show the total rates in the appearance channels $\nu_e \to \nu_\mu$ (left) and $\bar{\nu}_e \to \bar{\nu}_\mu$ (right) for $\Delta m^2_{21} = 0$ (solid line) and compare them with the total rates for $\Delta m^2_{21} = 10^{-4}$ eV ^{2} and four possible values of δ, $\delta = 0,\ \pi/2,\ \pi,\ 3\pi/2$ (dashed lines). Figure 8 corresponds to $\sin^2 2\theta_{13} = 0.01$. The relative magnitude of the Δm^2_{21} effects

[h] For $\Delta m^2_{31} = 7.0 \times 10^{-3}$ eV ^{2}, the same conclusions hold for approximately two times higher neutrino energies.

[i] For a rather detailed discussion of the dependence of the results presented above on the value of Δm^2_{31} see [3].

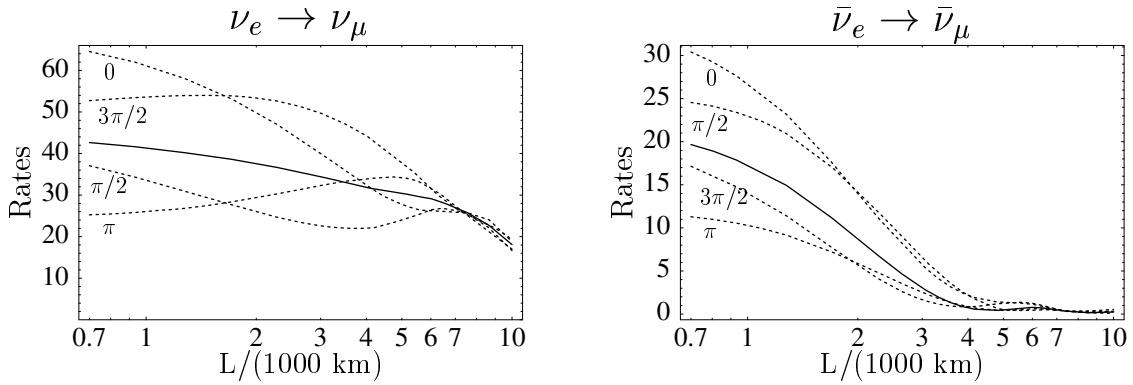

Figure 8: Appearance event rates $n_{\mu^+}(\mu^-)$, $n_{\mu^-}(\mu^+)$ in matter as functions of L for $\Delta m^2_{21} = 10^{-4}$ eV ^{2} and four possible values of the CP-phase $\delta = 0,\ \pi/2,\ \pi,\ 3\pi/2$ (dashed lines), compared with the corresponding event rates for $\Delta m^2_{21} \ll 10^{-4}$ eV ^{2} (solid lines). Both figures correspond to $N_\mu N_{\rm kT}\epsilon = 10^{21}$, $E_\mu = 20\,{\rm GeV}$, $\sin^2 2\theta_{23} = 1$, $\Delta m^2_{31} = 3.5 \cdot 10^{-3}$ eV^2, $\sin^2 2\theta_{12} = 0.8$ and $\sin^2 2\theta_{13} = 0.01$.

depends crucially on the value of θ_{13}: it grows when θ_{13} gets smaller [17,3] (compare Figs. 10 and 11 in [3]). This is because the zeroth order approximations (in Δm^2_{21}) for the appearance probabilities have a $\sin^2 2\theta_{13}$ suppression, whereas the linear Δm^2_{21} corrections (CP-conserving and violating) are suppressed by only one power of $\sin 2\theta_{13}$ (see eqs. (15) and (23)) and the corrections quadratic in Δm^2_{21} (CP-conserving) are not suppressed by θ_{13} at all. Indeed, at sufficiently small L we have $\sin(\Delta\bar{E}_m L/2) \cong \Delta\bar{E}_m L/2$, $\sin(\bar{\kappa}+\Delta\bar{E}_m L/2) \cong (\bar{\kappa}+\Delta\bar{E}_m L/2)$, etc., and as can be shown [3], the leading CP-conserving and CP-violating $\Delta m^2_{21}-$corrections containing the factor $\cos\theta'_{12}$ in eq. (23) reduce essentially to their vacuum oscillation form:

$$\Delta P^{3\nu}_E(\nu_e \to \nu_\mu;\ \delta) \cong \quad 8 J^V_{CP} \left(\frac{L}{2}\frac{\Delta m^2_{21}}{2E}\right) \left(\frac{L}{2}\frac{\Delta m^2_{31}}{2E}\right) \quad \left[\cot\delta \ - \ \frac{L}{2}\frac{\Delta m^2_{31}}{2E}\right] \tag{31}$$

where

$$J^V_{CP} = \frac{1}{8}\sin\delta\ c_{13}\sin 2\theta_{12}\sin 2\theta_{13}\sin 2\theta_{23} \tag{32}$$

is the CP-violation rephasing invariant of the lepton mixing matrix [42].

As we have indicated, the range of the Δm^2_{21} corrections is essentially determined by θ_{13}, but the precise size and sign of these corrections within this range is unknown if δ is unconstrained , as Fig. 8 shows. The Δm^2_{21} effects represent consequently in the present LMA scenario in a high statistics long-but-not-too-long baseline measurement of θ_{13} an important source of "systematic error", unless δ is measured [17,3]. By comparing, e.g., the left and right plots of in Fig. 8 one can see that, as it follows from eq. (23), the Δm^2_{21} correction has the same sign in the two channels for the two CP-conserving values $\delta = 0,\ \pi$, when $\sin\delta = 0$, but has opposite sign for the two CP-violating values $\delta = \pi/2,\ 3\pi/2$. Figure 8 shows also that the Δm^2_{21} effects become smaller when L increases and are essentially negligible at $L \gtrsim 7000$ km.

A measurement of δ, based on a comparison of CP-conjugated rates at a single L could not be enough in order to allow to determine unambiguously both the value of θ_{13} and that of δ. Suppose, e.g., that $\delta = 0$ or $\delta = \pi$. Then the Δm^2_{21} effects would be the same in the two channels and an ideal experiment looking for CP-violation would measure $\sin\delta = 0$. The value of δ would still be undetermined, however, since both $\delta = 0$ and $\delta = \pi$ give $\sin\delta = 0$. As a consequence, it would be still unknown whether the Δm^2_{21} corrections in both channels add ($\delta = 0$) or subtract ($\delta = \pi$) to the leading Δm^2_{31} contribution to the rates and this ambiguity would translate, e.g., in an uncertainty on a measurement of θ_{13}. Similar conclusion remains valid for $\delta \neq 0$ or π. Such an ambiguity could be resolved by comparing rates measured at different distances L [3]. Figure 8 shows that for $\sin^2 2\theta_{13} = 0.01$, the change in rates in the $\nu_e \to \nu_\mu$ channel between, e.g., $L = 3000$ km and $L = 7000$ km allows to discriminate between, e.g., $\delta = 0$ and $\delta = \pi$, or between $\delta = \pi/2$ and $\delta = 3\pi/2$.

The indicated problem was further studied in [21,22,23]. These studies, in particular, confirmed the conclusion [3] about the necessity to perform appearance experiments at two distances, at $L \sim 3000$ km and $L \sim 7000$ km, for resolving the ambiguities in the simultaneous determination of θ_{13} and δ from the total event rate data.

6. Matter Effects in the Energy Spectrum.

As we have discussed, statistical significant deviations from the appearance total event rates in vacuum represent already a good test of the MSW theory. A more detailed test could be performed by a sufficiently precise measurement of the neutrino energy spectrum, which is modified by the matter effects in a very characteristic way (Fig. 9). In the limit of $\Delta m^2_{21} = 0$, for instance, matter effects have no influence on the angle θ_{23}, whereas they modify the mixing due to θ_{13} significantly. The enhancement of θ^m_{13} is maximal in the neutrino channel when the neutrino energy E coincides with the MSW resonance energy $E_{\rm res}$, $E_{\rm res} = \Delta m^2_{31}\cos 2\theta_{13}/(2V)$. The maximum of the event spectrum in the $\nu_e \to \nu_\mu$ channel does not coincide, in general, with $E_{\rm res}$ since the MSW probabilities are folded with the fluxes and cross sections. The resulting maximum is for the muon energies under consideration still around $E_{\rm res}$ [3]. The $\nu_\mu \to \nu_\mu$ and $\bar\nu_\mu \to \bar\nu_\mu$ disappearance channels are dominated by transitions to ν_τ and $\bar\nu_\tau$, in which the matter effects play essentially no role. Thus, the differential event rate spectra corresponding to these channels are rather insensitive to matter effects.

The MSW effect changes the $\nu_e \to \nu_\mu$ transition probability compared to vacuum in three genuine ways: the first maximum of the oscillation probability as the energy decreases is enhanced, its width is broadened and its center is shifted to lower energies. Similarly one has an "anti–MSW effect" in the antineutrino appearance channel which implies for the first oscillation maximum a reduction in height, again a broadening and a shift to lower energies. These "genuine MSW effects" are demonstrated in Fig. 9 for $E_\mu = 20\,\text{GeV}$, showing the modifications in the energy spectrum due to

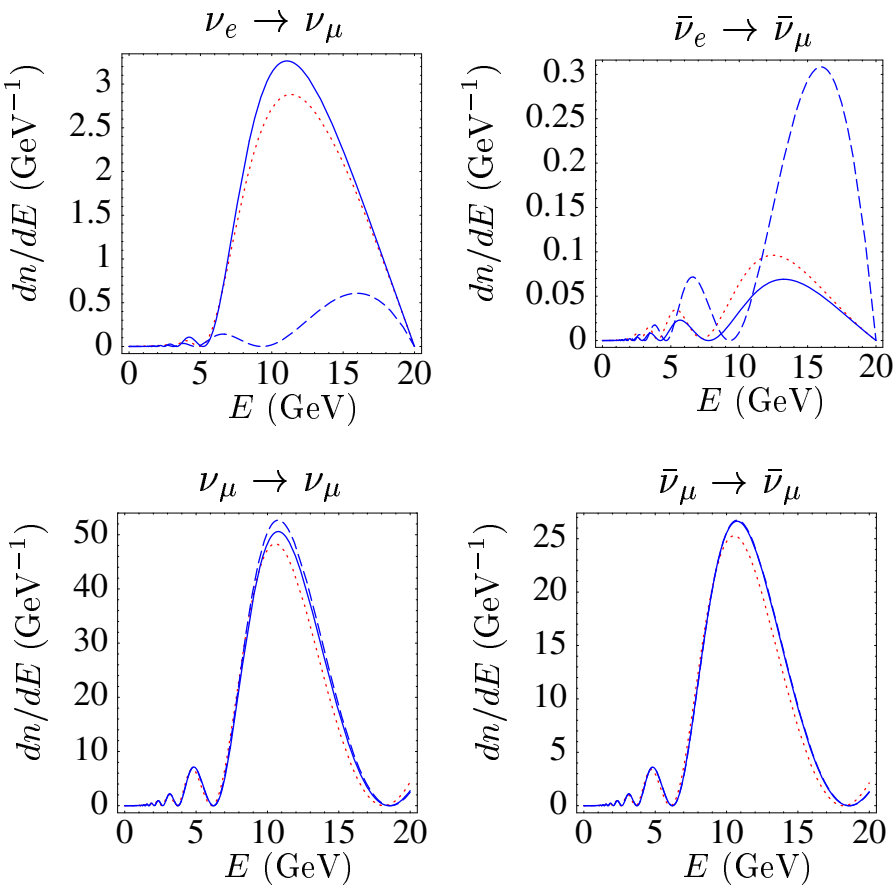

Figure 9: Modifications in the differential event rate spectrum (events per GeV) due to matter effects for $E_\mu = 20\,\mathrm{GeV}$. The solid lines correspond to oscillations in the Earth mantle, while the dashed lines are for oscillations in vacuum, with $\Delta m^2_{21} = 0$ in both cases. The "enhancement", the "broadening" and the "shift" of the first oscillation maximum in the $\nu_e \to \nu_\mu$ channel as E decreases, caused by the MSW effect, is clearly seen. The dotted lines show an example of Δm^2_{21} corrections for $\Delta m^2_{21} = 10^{-4}$ eV^2, $\delta = 0$ and $\sin^2 2\theta_{12} = 0.8$. The assumed parameters are in all cases $N_\mu N_{\mathrm{kT}} \epsilon = 10^{21}$, $L = 6596$ km (CERN-MINOS), $\Delta m^2_{31} = 3.5 \cdot 10^{-3}$ eV^2 and $\sin^2 2\theta_{13} = 0.01$.

matter effects. Figure 9 shows all effects due to the MSW mechanism, indicated above. As already observed in the previous section, the Δm^2_{21} corrections shown also in Fig. 9 (dotted lines, $\Delta m^2_{21} = 10^{-4}$ eV ^{2}, $\sin^2 2\theta_{12} = 0.8$) are relatively small for the very long baselines. For higher muon energy, e.g., for $E_\mu = 50\,\mathrm{GeV}$ (see Fig. 13 in [3]), the beam energy is already rather far away from the MSW resonance energy and the genuine matter effects would be somewhat harder to distinguish [3]. In any case, the measurement of the differential event rate spectrum could provide the extremely valuable possibility to test in detail the MSW theory.

7. Conclusions

The study performed within the framework of three-neutrino mixing in [3] shows

that the predictions of the MSW theory can be tested in a statistically reliable way in a large region of the corresponding parameter space by a simple analysis of the total "wrong sign" (i.e., appearance) muon event rates in a very long baseline neutrino oscillation experiment at a neutrino factory. This can allow to determine the sign of Δm^2_{31} as well. Not seeing the matter effects would lead to impressive upper limits on the mixing angle θ_{13} down to $\sin^2 2\theta_{13} \simeq (10^{-3} - 10^{-4})$ or even better.

Our analysis [3] showed that a higher sensitivity to the MSW effect in the case of relatively small values of $\sin^2 2\theta_{13}$ is achieved at rather large L, $L \sim (6000 - 7000)$ km. This conclusion holds also when subleading Δm^2_{21} effects are included. These effects can be significant in the case of the LMA MSW solution with $\Delta m^2_{21} \cong (0.5 - 8.0) \times 10^{-4}$ eV^2. At very large L, $L \gtrsim 7000$ km, the indicated Δm^2_{21}-induced effects are essentially negligible if $\Delta m^2_{21} \lesssim 3.0 \times 10^{-4}$ eV^2. For shorter baselines, Δm^2_{21} effects are non-negligible. The L dependence of the Δm^2_{21} effects offers the possibility to determine the CP-phase δ and the lepton mixing angle θ_{13} even when $\sin\delta$ is rather small. For $\sin^2 2\theta_{13} = 0.01$, for instance, the event rates due to the $\nu_e \to \nu_\mu$ and $\bar{\nu}_e \to \bar{\nu}_\mu$ transitions change considerably when L changes from to ~ 3000 km to ~ 7000 km. Thus, a measurement of these rates, at two distances, at ~ 3000 km and ~ 7000 km, could allow to determine simultaneously the values of θ_{13} and of δ with a certain precision and to study the matter effects in the neutrino transitions. Similar conclusion is reached in the recent more detailed studies [21,22,23]. The matter effects lead to a very characteristic distortion of the differential event spectrum of the "wrong sign" muon events. The observation of these distortions would allow very detailed tests of the MSW theory.

8. References

1) L. Wolfenstein, Phys. Rev. D17 (1978) 2369; S.P. Mikheyev and A.Yu. Smirnov, Sov. J. Nucl. Phys. 42 (1985) 913; V. Barger et al., Phys. Rev. D22 (1980) 2718.
2) B. Pontecorvo, Zh. Eksp. Teor. Fiz. 53 (1967) 1717.
3) M. Freund et al., Nucl. Phys. B578 (2000) 27.
4) S. Geer, Phys. Rev. D57 (1998) 6989, (E) *ibid.* D59 (1999) 039903.
5) Y. Takeuchi (Super-Kamiokande Coll.), these Proceedings.
6) M.C. Gonzalez-Garcia et al., Phys. Rev. D63 (2001) 033005.
7) G.L. Fogli et al., these Proceedings.
8) C. McGrew (Super-Kamiokande Coll.), these Proceedings.
9) S.T. Petcov, Phys. Lett. B434 (1998) 321; M.V. Chizhov and S. T. Petcov, Phys. Rev. Lett. 83 (1999) 1906 and Phys. Rev. D63 (2001) 073003.
10) P. Lipari, Phys. Rev. D61 (2000) 11304; V. Barger et al., Phys. Rev. D62 (2000) 013004.
11) S.M. Bilenky, S. Pascoli and S.T. Petcov, hep-ph/0102265.

12) M. Appolonio et al., Phys. Lett. B466 415 (1999) 415.
13) S.M. Bilenky et al., Phys. Rev. D54 (1996) 4432.
14) A. Bueno, M. Campanelli and A. Rubbia, Nucl. Phys. B589 (2000) 577.
15) P. Di Bari et al., hep-ph/0008245; A.D. Dolgov, hep-ph/0004032.
16) A. De Rujula, M.B. Gavela and P. Hernandez, Nucl. Phys. B547 (1999) 21.
17) K. Dick et al., Nucl. Phys. B562 (1999) 29.
18) V. Barger, S. Geer and K. Whisnant, Phys. Rev. D61 (2000) 053004.
19) A. Donini et al, Nucl. Phys. B574 (2000) 23; A. Romanino, Nucl. Phys. B574 (2000) 675.
20) A. Cervera et al., Nucl. Phys. B579 (2000) 17.
21) P. Hernandez, these Proceedings; J. Burguet-Castell et al., hep-ph/0103258.
22) M. Freund, P. Hubner and M. Lindner, hep-ph/0105071.
23) J. Pinney and O. Yasuda, hep-ph/0105087.
24) Proceedings of the NuFACT '99 Workshop, July 5–9th, Lyon, Nucl. Instrum. Meth. Phys. A451 (2000): see, e.g., A. Blondel et al., p. 102.
25) F.D. Stacey, *Physics of the Earth*, John Wiley and Sons, New York, 1977; A.D. Dziewonski and D.L. Anderson, Phys. Earth Planet. Interiors 25 (1981) 297.
26) M. Maris, Q.Y. Liu and S.T. Petcov, study performed in December of 1996 (unpublished).
27) M. Freund and T. Ohlsson, hep-ph/9909501; I. Mocioiu and R. Shrock, hep-ph/9910554.
28) M. Maris and S.T. Petcov, Phys. Rev. D56 (1997) 7444.
29) A. Cervera, F. Dydak and J.J.G. Cadenas, Nucl. Instrum. Meth. Phys. A451 (2000) 123.
30) A. De Rujula et al., Nucl. Phys. B168 (1980) 54.
31) S.M. Bilenky and S.T. Petcov, Rev. Mod. Phys. 59 (1987) 671.
32) F. Boehm, J. Busenitz et al., Phys. Rev. Lett. 84 (2000) 3764.
33) S.T. Petcov, Phys. Lett. B214 (1988) 259; P.I. Krastev and S.T. Petcov, Phys. Lett. B299 (1993) 99.
34) C.-S. Lim, Report BNL 52079 (1987).
35) S.T. Petcov, Phys. Lett. B 200 (1988) 373, *ibid.* B214 (1988) 139 and B406 (1997) 355.
36) S.T. Petcov, Lecture Notes in Physics, 512 (1998) 281.
37) E. Lisi et al., Phys. Rev. D63 (2001) 093002.
38) M. V. Chizhov, M. Maris and S. T. Petcov, hep-ph/9810501.
39) O. Yasuda, hep-ph/9910428.
40) M. Freund, hep-ph/0103300.
41) C. Caso et al., European Phys. J. C3 (1998) 1.
42) P.I. Krastev and S.T. Petcov, Phys. Lett. B205 (1988) 84.
43) P.K. Kuo and J. Pantaleone, Phys. Lett. B198 (1987) 406.